

## THEME ORIENTED ENHANCEMENT OF SEA SURFACE TEMPERATURE IN THERMAL INFRARED AVHRR IMAGES

M.R. Ramesh Kumar, R.K. Gupta<sup>1</sup> and V. Dayal<sup>2</sup>

*National Institute of Oceanography, Dona Paula, Goa-403004*

### ABSTRACT

The paper provides a brief description of NOAA satellite AVHRR (Advanced Very High Resolution Radiometer) and also the concept of theme oriented enhancements and touches upon the efforts deployed in developing the software module for its realisation under project INTERACT (International Education and Research for Application of Computer Technology). The paper provides the details of one of the eighteen enhancement curves implemented and which refers to the sea surface temperature. The enhanced output image and comparison of the brightness temperature values of the enhanced portion of the image with the sea surface temperature values available from other sources have been discussed.

### INTRODUCTION

The Advanced Very High Resolution Radiometer (AVHRR) onboard NOAA series of polar orbiting meteorological satellites provides 1.1 km sub satellite point (SSP) resolution digital data in 0.55-0.68 (visible), 0.725-1.1 (near infrared (NIR)), 3.55-3.93 (middle IR, Channel 3), 10.3-11.3 (thermal IRI, Channel 4) and 11.5-12.5 (thermal IR2, Channel 5) micron spectral bands. These data sets are basically useful in generating the images of lower boundary (as seen from satellite altitude) which could be oceans, land-mass features including snow and different types of clouds. The 10-bit on-board quantization of the data provides 1024 gray scales in the data sets. The display capacity of COMTAL 8000R Image processing system for 256 gray levels restricts the display of images to 8-bit resolution by compressing the original 10-bit data to 8-bit representation. The eye-brain system is credited with the ability to discriminate among hundreds of gray levels and 20,000 or more colours (Strandberg, 1967; Heller, 1970). However according to Garner (1962) an average human can identify only 5 gray-level categories and 11 hues (saturated) when viewing isolated panels. As the colour receptors in the eye are connected by a complex feedback network the human eye is able to see slight changes across sharp boundaries in colour images (Cornsweet, 1970). The gray scales in the Black and White satellite images are limited to

about seventeen. If one is interested in better representation of a limited portion of gray levels with slight degraded representation of other grey levels, the image generation could be carried out by applying a set of non linear transformations while mapping the actual gray level in the output image. The main objective of image enhancement is to process a given image so that the result is more suitable than the original image for a specific area of application (Chatterji, 1984). These developed image enhancements are different from the general purpose image processing enhancements like gray level stretching, histogram equalisation, convolution etc. available on commercial image processing systems as these are sensor and spectral band specific and pertain to the generation of Look-up Table Definition Function (LTDF) for different applications aim (herein developed for 18 applications). LTDF creation is carried out through a series of software modules and user only needs to give the temperature ranges of interests and the stretching code; stretching code provides user's choice to select one of the grey scale interpolation technique (during LTDF creation) out of linear, logarithmic, exponential, square root and tangential modes in accordance with the expected physical process nature - this user freedom is available for each segment of a particular application LTDF. With the change in the spectral filter response function of spectral band(s) either due to launch

1. National Remote Sensing Agency, Hyderabad  
2. India Meteorological Department, New Delhi

of different satellite or due to degradation of sensor with time, user could generate new LTDF just by reissuing command for executing the software package. The study reported here emerged from the project activities (Dayal et al; 1984) carried out under the project INTERACT.

## METHODOLOGY AND SOFTWARE DEVELOPMENT:

The AVHRR data pertaining to the NOAA-7 satellite generated by National Remote Sensing Agency, Hyderabad, using the High Resolution Picture Transmission (HRPT) format was used in the study. The digital analysis facilities built up under the project - named CIPSMAP (Computerised Image Processing System for Meteorological Applications) - were used; a brief account of CIPSMAP is available in Gupta and Murthy (1985).

Figure 1 gives the conceptual basis of theme oriented enhancements. The curve OA represents the one to one linear mapping between actual input count and the output count (the transformed count as displayed in the image). Here the slope of the line OA is unity. The curve OBB refers to the segment OB where the

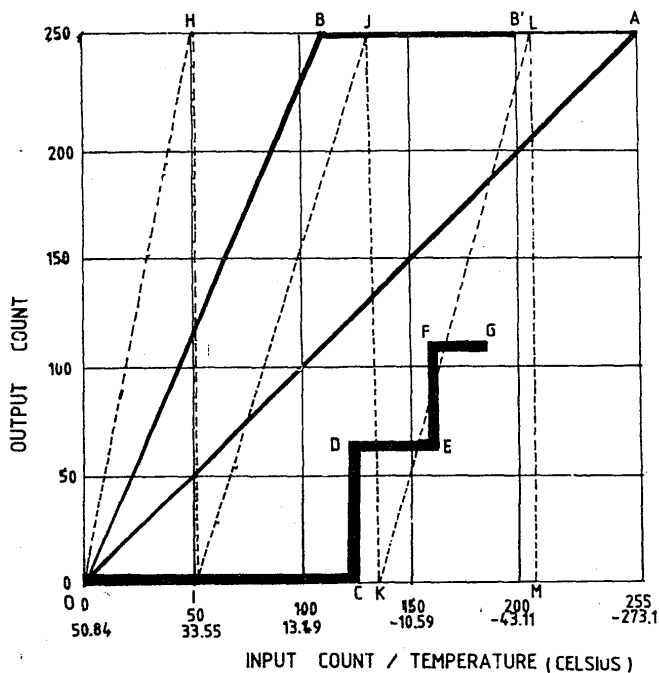


Fig. 1. Conceptual representation of the theme oriented enhancement technique for thermal infrared data.

slope is greater than unity in the segment OB and the slope is zero in the segment BB' implying the masking of information gradient in the input count range corresponding to segment BB'. O-C-D-E-F-G involves assigning of a particular output count to a range of input counts (thus masking the gradient) and represents step function enhancement. All these enhancements are to improve the representation of small temperature gradients.

The steep linear (slope greater than one) enhancing technique provides excellent details in the data. With multiple linear enhancements (curve O-H-I-J-K-L-M) one could obtain increased contrast for the whole temperature range but the resulting introduction of multiple grey scales may mask meteorologically significant cloud edges. The step function enhancements are useful for bringing out the vertical structure of clouds.

Improved interpreting for the enhanced images demands observing of following criteria:

a) Number of features to be enhanced in a image should be limited.

b) Only necessary details in the data should be studied, without making the display overlay confusing.

Each image contains informations on a variety of features related to oceans, landmasses including snow and clouds. All these features can not be enhanced simultaneously by a single enhancement curve. In other words one can enhance the features of one's interest by suppressing other features. Thus one has to trade off between the number of features to be enhanced and the easiness in assimilation.

A total set of 18 enhancement curves for the themes of snow, ocean, landmass features, low, middle and high cloud combinations; for tropical cyclone and other weather systems based on the temperature climatologies for the features as used for GOES satellites (Clark, 1983) were developed.

The enhancement studies draw significant information from the temperature of the objects available through the VHRR thermal channel in the range 10.3-11.3  $\mu\text{m}$ .

In NOAA7/AVHRR there are three thermal channels in 3.55-3.93 (channel 3), 10.3-11.3 (channel 4) and 11.5-12.5 (Channel 5)  $\mu\text{m}$ . The effect of uncertainties or errors in the Planck function ( $\Delta B/B$ ) on the accuracy of sea surface brightness temperature ( $\Delta T_s$ ) could be expressed as (Chahine, 1980).

$$\Delta T_s = \left[ \frac{T_s^2 (1 - e^{-c_2/T})}{C_2 \gamma} \right] \frac{\Delta B}{B}$$

$C_2$  being one of the planck function constant. For a given error  $\Delta B/B$ , the  $\Delta T_s$  would be larger for  $\gamma = 900 \text{ cm}^{-1}$  than for  $\gamma = 2500 \text{ cm}^{-1}$  making 3.7  $\mu\text{m}$  window more advantageous compared to 11  $\mu\text{m}$  window. Further, channel 3 is more sensitive to warm, temperature regions as compared to other two thermal IR channels because this channel lies on an exponential end of a black body curve. Thus it can not be used for identifying the temperature information for the whole constituent of low-, middle- and high-level clouds. In addition to this, the solar energy reflected and emitted from clouds will be comparable in magnitude to the channel 3 information. This makes channel 3 useful only during night time.

Water vapour has continuum as well as line absorption effects in the 10.3-12.5 micron spectral thermal IR window channels. Absorption by water vapour is a function of its amount and partial pressure. Dependence of absorption on partial pressure and temperature has lead to the concept of absorption by dimers i.e.  $(\text{H}_2\text{O})_2$  - these aspects have been reviewed in Gupta (1978). Split window 10.3 - 11.3 and 11.5 - 12.5 micron channels provide the advantage of correcting for atmospheric (including water vapour) effects as the optical thickness terms would be

different in these split window concept for improving sea surface temperature ( $T_s$ ) estimation by adding a weighted value of AVHRR Channel 4 ( $T_4$ ) and AVHRR Channel 5 ( $T_5$ ) brightness temperatures difference to base  $T_4$  brightness temperature as illustrated by

$$T_s = T_4 + 2.705 (T_4 - T_5) - 0.578$$

Fig. 2 (after Phulpin and Dechamps, 1980) gives a graphic idea of 11 and 12  $\mu\text{m}$  window channels total transmittance value variation as a function of integrated water-vapour content of atmosphere ( $x$ ) for Zenith angle values of  $0^\circ$  and  $45^\circ$ . It could be seen that total transmittance for 11  $\mu\text{m}$  channel is always higher as compared to 12  $\mu\text{m}$  channel where water vapour absorption effect is comparatively higher. One more interesting feature seen is that for 12  $\mu\text{m}$  (AVHRR channel 5) one could fit in a linear approximation (C) given by  $t = 1 - 0.15x$  upto 5  $\text{g}/\text{cm}^2$  while for AVHRR channel 4 such linear approximation has to be different for low water-vapour case (A) given by  $t = 1 - 0.08x$  and for high water-vapour content case (C) given by  $t = 1 - 0.11x$ . This demonstrates that AVHRR channel 4 is less affected by water-vapour as compared to AVHRR channel 5 and need to be considered as base value for this reason and for the reason of having different linear approximations in low and high water vapour content situations. Hence the reported study was undertaken using AVHRR channel 4 data.

The sea surface enhancement curve was implemented as shown in figure 3 and the table 1 gives the input-output counts transformation details for the thermal IR channel no. 4.

The first process for implementation had been the conversion of count values of the channels into brightness temperature values which first needed the computation of calibration coefficient using the calibration data available in the data stream. The calibration process is two point calibration and has been implemented in CIPSMAP as per procedures laid down by US NOAA/NESDIS.

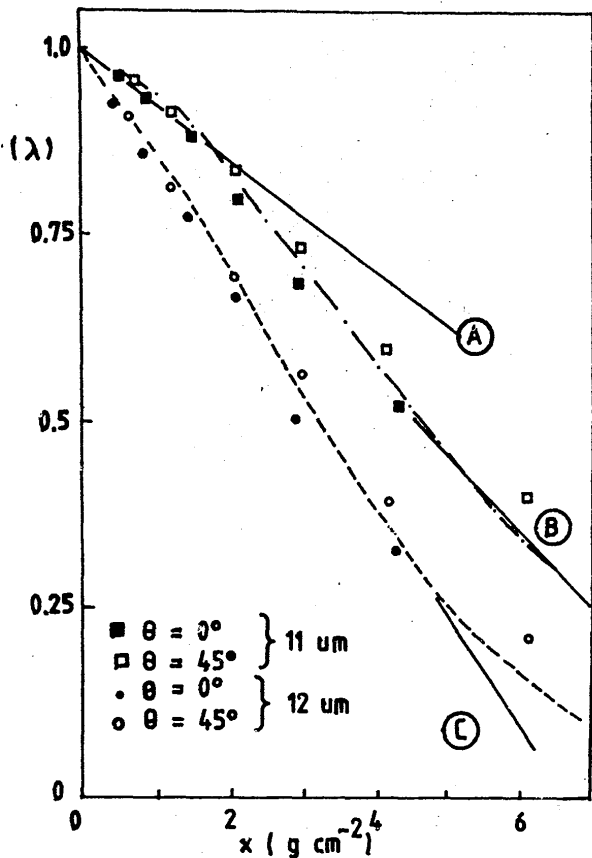


Fig. 2. Total transmittances  $t$  at 11 and 12  $\mu\text{m}$  as a function of integrated water-vapour content  $x$  (after Phulpin and Deschamps 1980), 0 is the zenith angle. Linear approximations: (A)  $t = 1 - 0.08x$  (11  $\mu\text{m}$ , low water-vapour content), (B)  $t = 1 - 0.11x$  (11  $\mu\text{m}$  high water-vapour content) and (C)  $t = 1 - 0.15x$  (12  $\mu\text{m}$ ).

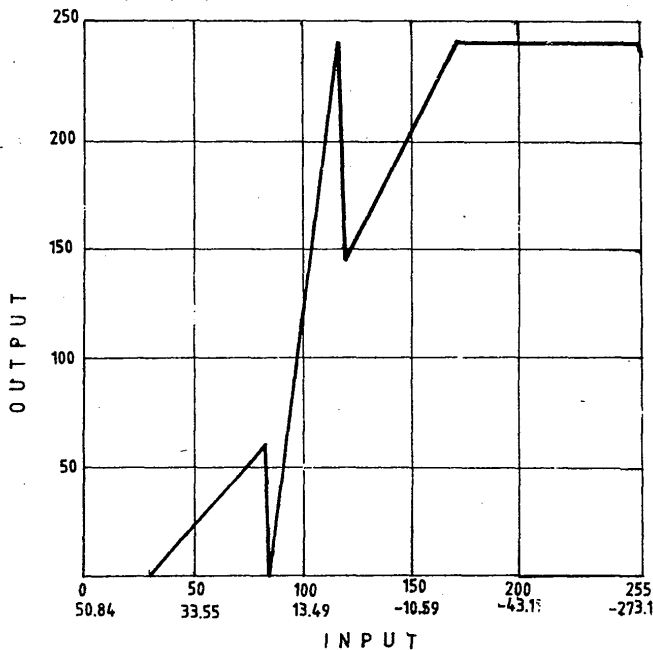


Fig. 3. The graphic representation of the Sea surface temperature enhancement curve for NOAA/AVHRR 10.3-11.5  $\mu\text{m}$  thermal IR channel.

Basically it is a linear relationship of the following form,

$$\text{Radiance (B)} = \text{Gain} \times \text{Count} + \text{Intercept}$$

To compute two unknowns, namely 'Gain' and 'Intercept', the satellite provides count value for space and internal target onboard the satellite. The radiance for internal target is computed by calibration program, using the temperature information of target (provided by the satellite) and the filter function characteristics for each of mid, thermal IRI and thermal IR2 channels. Radiance for space is assumed to be zero.

With the 'Gain' and 'Intercept' for thermal IR, channel 4, available as a output of developed calibration program, one can compute the radiances in channel 4 for the whole 10-bit count range (0-1023). Planck's function relates these radiances (B) with the surface brightness temperature ( $T_s$ °K) in the following way:

$$B(\gamma T_s) = \frac{C_1 \cdot \gamma^3}{(e^{C_2 \cdot \gamma/T_s} - 1)}$$

Where  $\gamma$  is the channel wave number and

$$C_1 = 1.1910659E-5$$

$$C_2 = 1.438833$$

From the above equation  $T_s$  can be computed.

For this computation,  $\gamma$  was taken as the central weighted frequency of the filter.

A computer program to compute temperatures was developed and implemented. This can generate table for brightness temperature with 6, 8 and 10 bit precision in degrees Kelvin or degrees Centigrade.

The figure 3 has been generated with a prior information on temperature range and corresponding output count range. A program to read

the temperature range for a given curve and to find out the corresponding input count range by applying binary search process to the count-to-temperature tables pertaining to a given satellite for a specific channel (all these flexibilities have been incorporated in the software module for the theme oriented enhancement has been developed. Thereafter a set of another program takes the output of binary search program as input and finally generates a table between input and output count ranges with associated tags in file names to specify the satellite, channel number, enhancement curve number and the stretching code so that the function processing memory of COMTAL 8000R work station could be loaded. The display of image with activated function memory provides the enhanced image on the display device. Hard copy could be generated for the so enhanced image by exposing the film to the display or by transferring it to a dot matrix printer through a dithering program which reduces the grey levels from 255 (on display) to 36 on dot matrix printer. The original image picture at figure 4 addresses to the 18 April 1983 afternoon NOAA meteorological satellite pass data in AVHRR channel 4, the artificial delineation with white ink has been made to mark the land mass in this dithered which is a portion of Arab land (marked A in the picture at figure 6—the remaining area in figure 4 is Arabian sea. applying the enhancement curve (graphically described at figure 3) through developed software the image got enhanced and its dithered output is available at figure 5. Various segments of the data set were enhanced similarly and figure 6 depicts their mosaic. Use of video monitor provides better grey level resolution and was used as monitor. Dithered output on matrix printer served as the quick hard copy output and brought out considerable contrast to meet the herein discussed application needs.

## ANALYSIS

Figure 6 depicts the enhanced satellite imagery for the Arabian Sea and Persian Gulf area of NOAA 7/AVHRR, Channel 4, Orbit 9373, on 18th April 1983. This picture was enhanced by using the curve shown in figure 3. The original

picture did not show any visible difference in the grey shades over this area. The enhancement of this Arabian Sea area has brought out lot of features and these were not even noticeable in the original image. Figure 7 gives the satellite derived, Global Operational Sea Surface Temperature Computation (GOSSTCOMP) chart for 19th April 1983. Even though the most of the features are the same in both the pictures the enhanced version gives much more detailed information like warm eddies (marked B in figure 5) etc. The Persian Gulf area is quite cold as compared to the northern Arabian Sea. These cold waters seem to spread to the west coast of India. The warmest waters (marked C in figure 5) are observed in the central Arabian Sea region. There is another cold patch region near the Arabian coast (marked D in figure 5).

The enhanced features in the Arabian Sea referred to counts range of 70 to 71 in a 8-bit range which could be related to 10-bit count range (actual dynamic range of data) 280 to 287 which in turn addresses to the temperature range of 25.73 to 25.07°C in region upto 30°N for the precipitable water range of 2.1 to 4.4 gm/Cm<sup>2</sup> (Table 2, after Maul G.A., 1985). These are based on the hemispheric averages and are for January and July months. It may be noted that Table 2 addresses to vertical viewing condition while the AVHRR image has  $\pm 55.4^\circ$  scan angle with respect to situation for subsatellite path passing through the centre of the image in across latitude direction. Figure 8 (after Maul and Sidran (1973) describes the effect of nadir angle changes (for space-borne Very High Resolution Radiometer) for a given set of Sea surface temperature having a difference range of 8°C. This 8°C difference of surface temperature leads to a difference of about 2.7°C at vertical viewing in satellite data based brightness temperature estimation which gets further reduced to 1.5°C at about 50° nadir angle. Though as per Table 2 one expects about 4.1°C atmospheric effects error in January month for hemispherically averaged vertical viewing conditions at 30°N latitude it is expected to become about 50% lower at high scan angles. Based on this and on the fact that mid-latitude is

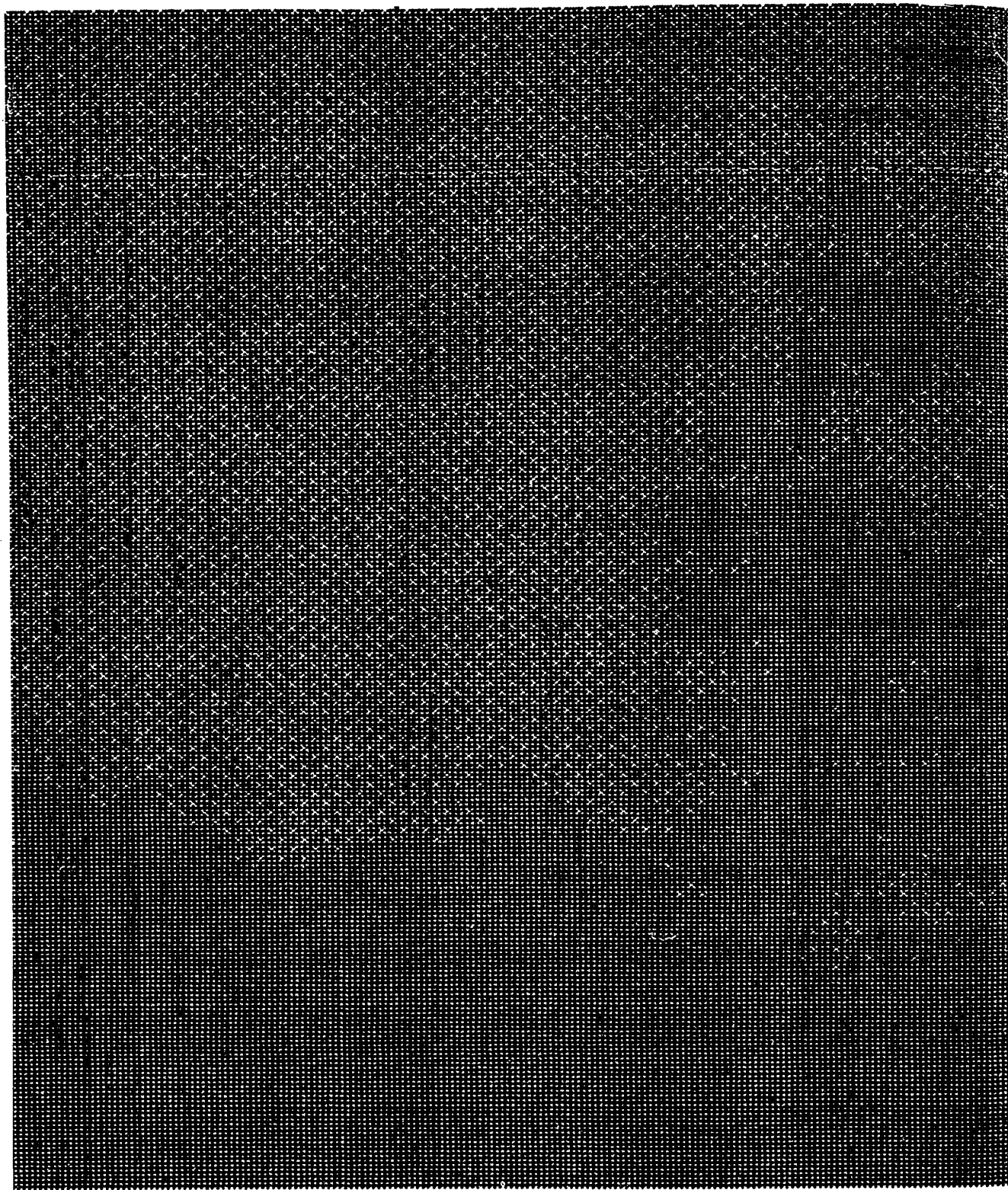


Figure 4 The dithered original image of Arabian sea and a part of the Arabian coast land mass extracted from NOAA meteorological satellite afternoon pass on 18 April 1983.

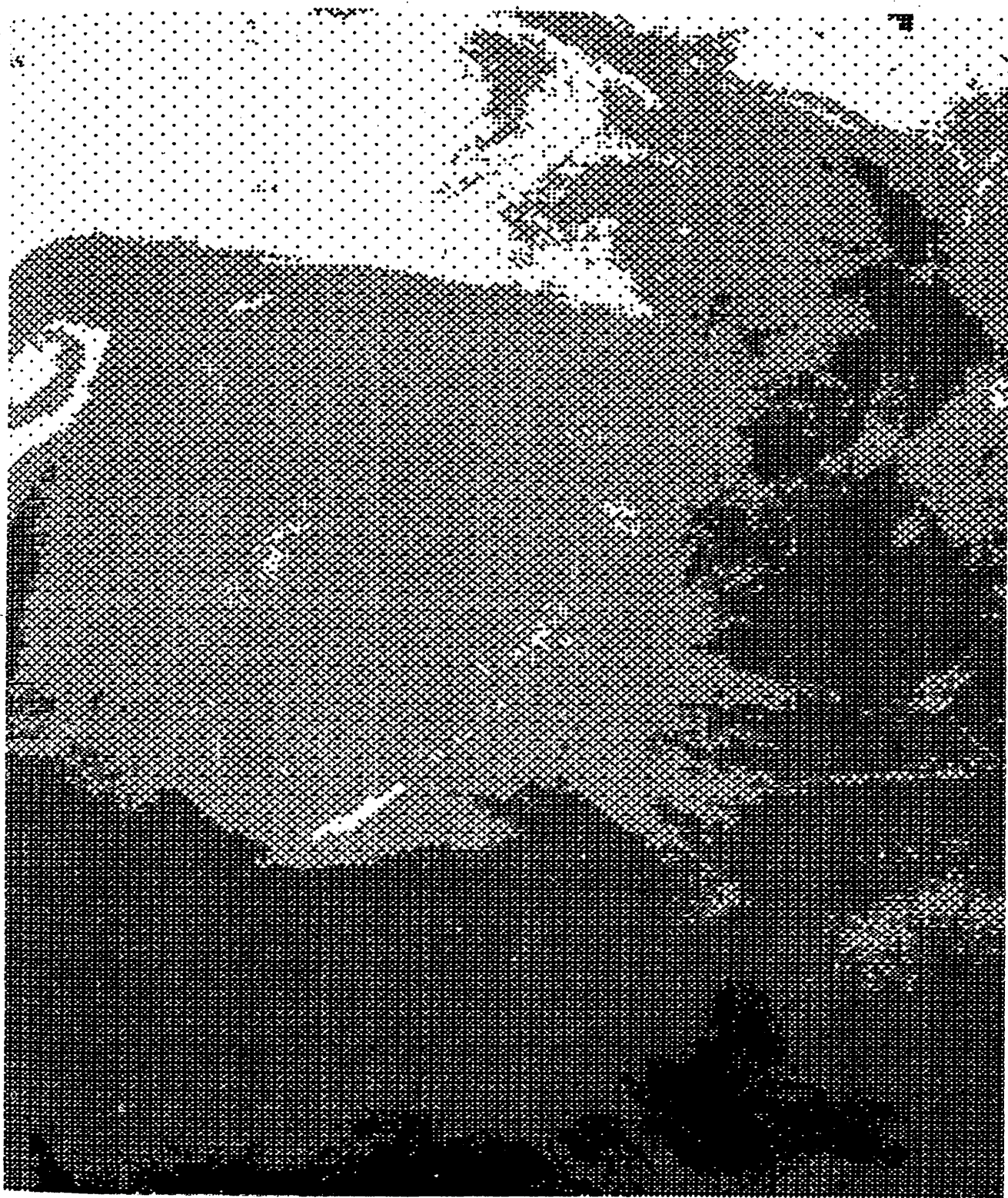


Figure 5 Sea surface brightness temperature information enhancement for the image at figure 3.



quite precipitation season in December through February (these are termed as western disturbances in the Indian region) while the figure 6 refers to April month, wherein convection activity is practically nil as could be seen from image itself, the observed deviation of 1 to 2°C in figure 6 from GOSSTCOMP is the expected error due to atmospheric effects.

## CONCLUSIONS

Theme oriented enhancement technique is a fast mode of assimilating information from the image with a predefined and preconceived transformation. As this is based on the physical temperature aspects, the interpretability could be a fast process once the user has acquired some experience in handling the data.

The common features of the enhancement curves is that they consist of two fundamental enhancements, namely linear stretching for a given input count range with various values of slope (slope = 1.0 means no enhancement) and a set of concatenated step functions.

The enhanced thermal structures over oceanic waters could not have been brought out in the synoptic view of unenhanced image. As the enhancement is through display modification by loading the function processing memory it takes very little time (practically negligible) to enhance the image which enables utilization in operational activities. The enhancement technique is thus useful in locating features like thermal fronts, eddies, upwelling zones, etc in the ocean.

## ACKNOWLEDGEMENT

The work was carried out under project INTERACT at Computer Maintenance Corporation, Secunderabad. Project INTERACT was funded by UNFSST, UNDP and Govt. of India. Authors are thankful to the Manager, project INTERACT, Director, National Institute of Oceanography, Director, National Remote Sensing Agency and Director General of Meteorology for the encouragement and support.

**TABLE 1** Input-output count transformation for theme oriented - enhancement of sea surface temperature

Channel number = 4 of AVHRR				Data type: 10 bit data			
S.No.	Segment No.	Starting temp.	Input count	Output count	Ending temp.	Input count	Output count
1	1	314.35	030	0	294.40	082	59
2	2	294.40	082	59	293.90	083	0
3	3	293.90	083	0	278.40	118	248
4	4	278.40	118	248	277.90	119	145
5	5	277.90	119	145	250.40	171	248
6	6	250.40	171	248	249.90	248	248

**TABLE -2** Atmospheric effects on infrared sea surface temperature sensing at 10-12 μm (From Maul GA, 1985)

Atmosphere	SST $T_s$ (K)	Calculated temperature at satellite $T_c$ (K)	Temperature departure $T_s - T_c$ (K)	Precipitable water (gm cm <sup>-2</sup> )
15°N Annual	299.6	291.0	8.6	4.0
30°N January	287.2	283.1	4.1	2.1
30°N July	301.2	290.6	10.5	4.4
45°N January	272.6	270.4	2.2	0.8
45°N July	294.2	287.7	6.4	3.0
60°N January	271.2	268.7	2.5	0.4
60°N July	287.2	281.6	5.6	2.1



NOAA-7/AVHRR CH#4 ORBIT 9373 DATE 18-APRIL 1983



Figure 6 Mosaic of dithered enhanced images of 18 April 1983 NOAA meteorological satellite afternoon pass over Arabian sea.

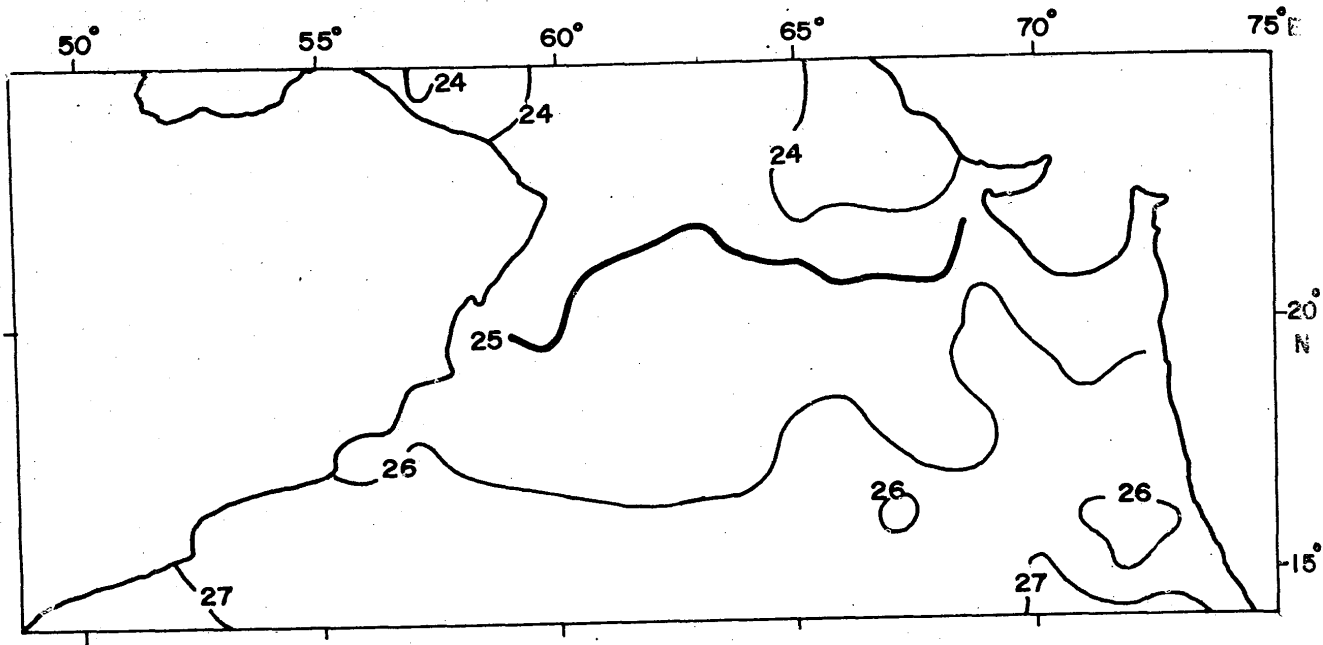


Figure 7 Satellite data derived (at NOAA/NESDIS) Global Operational Sea Surface Temperature Computation (GOSSTCOMP) chart for April 19 1983.

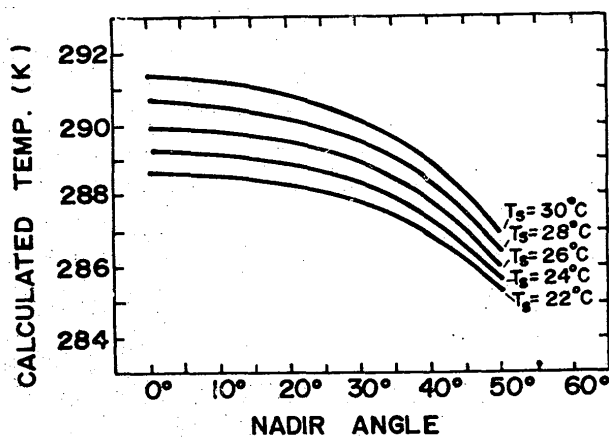


Figure 8 Effect of scan angle variation on sea surface temperature computation as a function of surface temperature for a warm moist atmosphere [From Maul and Sidran (1973)].

## REFERENCES

- Chahine M.T., 1980: Infrared Remote Sensing of Sea surface temperature, in Remote Sensing of Atmosphere and Oceans, Ed: A. Deepak, Academic Press, New York, 411-436.
- Chaterji B.N., 1984 Digital Picture processing, in Short term course on Digital image processing held at I.I.T Kharagpur from June 11-16.
- Clark, J.D., 1983: The GEOS User's Guide, US, NOAA/NESDIS, Washington, D.C. 20233, USA.
- Cornsweet Tom N. 1970: Visual Perception, New York, Academic Press.
- Dayal V, G. Neboja, M.R. Ramesh Kumar, C.K. Chandrasekharan, S. Budiman, U. Khin Than and R.K. Gupta, 1984, CIPSMAP Theme Oriented Enhancement Studies, Project INTERACT (second CIPSMAP training course activities), Computer Maintenance Corporation, 115 Sarojini Devi Road, Secunderabad 500003.
- Gupta R.K., 1978: Infrared remote temperature measurements: its physics with reference to complexities, approximations and limitations involved. I-Conceptual considerations and surface temperature estimation, J. Indian Institute of Science, 60(6), 135-169.
- Gupta R.K. and N.N. Murthy, 1985: Development of digital interactive processing system for NOAA satellites AVHRR data, Adv. Space Res; 5(6), 385-394.
- Heller Robert C., 1970: Imaging with photographic sensors, Chapter 2 in Remote sensing with special reference to Agriculture and Forestry. National Academy of Sciences, Washington, D.C. p 45.
- Maul G.A. and Sidran M., 1973: Atmospheric effects of Ocean surface temperature sensing from NOAA satellite scanning radiometer, Journal of Geophysical Research, 78 (12): 1909-1916.
- Maul G.A., 1985: Introduction to Satellite Oceanography, Martinus Nijhoff publishers, Dordrecht.
- McClain E.P., W.G. Pichel, C.C. Walton, Z. Ahmed and J.Sutton, 1983: Multichannel improvements to satellite-derived sea surface temperatures, Adv. Space Res., 2(6), 43-47.
- McMillin L.M., 1980: The split-window retrieval algorithm for sea surface temperature derived from satellite data, in Remote Sensing of Atmosphere and Oceans, Ed: A. Deepak, Academic Press, New York, 437-455.
- Phulpin T. and P.Y. Deschamps, 1980: Estimation of sea surface temperature from AVHRR infrared channel measurements, Procs. Sixth Annual Conf. of Remote Sensing Society, Ed: A. Cracknell, Dec. 18-19, 1979.
- Strandberg Carl H, 1967: Aerial Discovery Manual, New York: John Wiley and Sons.